Optoelectronic devices for optical chaos communications

Claudio R. Mirasso[a], Ingo Fischer[b], Laurent Larger[c]

[a] Electrical Engineering Department, 56-147C Engineering IV UCLA Los Angeles, CA 90095-1594; Permanent Address: Departament de Física, Universitat de les Illes Balears, E-07122 Palma de Mallorca, Spain
[b]Institute of Applied Physics, Darmstadt University of Technology, Schlossgartenstr. 7 D-64289 Darmstadt, Germany
[c] Laurent Larger, Laboratoire d'Optique P.M. Duffieux, Universit de Franche-Comt, UFR Sciences, route de Gray, 25030 Besanon cedex, France

ABSTRACT

We present results on the state-of-the-art in optoelectronic devices for chaos generation and message encryption. We concentrate on two kind of chaos based emitters and receivers: a semiconductor laser subject to all-optical feedback and operating in a non-linear regime and a semiconductor laser subject to non-linear electro-optical feedback and operating in a linear regime. We show that both configuration give very good synchronization properties and are suitable for message enconding at bit rates as high as Gbit/s.

Keywords: Synchronization, chaos, chaos encryption, optical communications, semiconductor lasers.

1. INTRODUCTION

The use of chaotic waveforms has been proposed as an alternative technique to encrypt information. The idea was introduced by Pecora and Carroll[1] based on the synchronization properties of two unidirectionally coupled chaotic systems, an it was implemented by Cuomo and Oppenheim.[2] Since these successful papers, it develops the possibility of applying such techniques to increase the privacy in the communications. The first experiments were carried out using electronic circuits. However, such systems present two disadvantages: on the one hand the maximum frequency for the chaotic carriers is some tens of KHz and, on the other hand, the dimensionality of the generated chaos is low (typically less than 3) allowing an easy interception and recovery of the message.

Most of these problems were overcome when working in the optical domain and by using delay optical feedback to generate chaotic carriers. Based on these ideas, it was numerically shown that a message could be encoded and decoded within a high dimensional chaotic carrier when using a pair of unidirectionally coupled single-mode semiconductor lasers subjected to coherent optical feedback.[3] Experimental results were later obtained for erbium doped fiber ring lasers[4] and semiconductor lasers.[5–8] Recently, it was shown that the system would also work when using incoherent optical feedback[9] or linear optoelectronic feedback.[10]

The success of the technique is based on the fact that two spatially separated chaotic semiconductor lasers are able to synchronize to each other. Synchronization means that the irregular output of the emitter device can be reproduced by the receiver. Once the two lasers have synchronized, the output light of the emitter can be used to encode a message. The latter has to have an amplitude small enough that it only slightly perturbs the chaotic carrier. It turns out that the receiver device synchronizes to the emitter carrier suppressing the encoded message. Consequently, by operating with the input and output of the receiver the message can be extracted.

In this work we review the main characteristics of the emitter/receiver devices concentrating in two kind of chaotic systems: a semiconductor laser subject to a delayed all-optical feedback and a semiconductor lasers subject to a delayed non-linear electro-optical feedback. While in the former the lasers operates in a non-linear regime, in the latter the laser operates in the linear regime. In both cases an hyper-chaotic carrier, i.e. a high dimensional chaotic attractor, is generated. This fact is essential to ensure privacy in the communication. It

---

Telephone: 34-971172783, Fax: 34-971173426, http://www.imedea.uib.es/Photonics,
E-mail addresses: claudio@galiota.uib.es, ingo.fischer@physik.tu-darmstadt.de, laurent.larger@univ-fcomte.fr

is well known that the higher the complexity of the chaotic carrier the more difficult is to decode the message without the appropriate receiver due to the high frequencies involved and the large number of degrees of freedom of the chaotic carrier. It is worth noting that chaotic carriers provide in semiconductor diode lasers a broad spectrum (typically in the 10-100 GHz range) in which the message can be hidden. The properties of these carrier signals, and the way the message is encoded, are such that with a linear filtering process it is not possible to extract the message. Also correlators and frequency-domain analysis would fail. In the section 2 we present the emitter/receiver systems operating in the all-optical feedback scheme; in section 3 emitter/receiver systems operating in the electro-optical feedback scheme and a summary and some conclusions are given in section 4.

2. EMITTER AND RECEIVERS SUBJECT TO ALL-OPTICAL FEEDBACK

The easiest way to produce chaotic light is by adding a mirror at the output of the laser, in our case a semiconductor laser. Figure 1 shows a schematic representation of an external cavity semiconductor laser (ECSL). The semiconductor laser (SL) with the facet reflectivities R1 and R2 is electronically pumped by a low noise current source with the injection current I_{DC}. The internal round trip time of the light is τ_{SL}. The emitted light is reflected from a distant mirror with the reflectivity R3 and reinjected into the SL with a time delay of τ_{delay}. Due to the small extension of the SL typically lying in the range of 500 m for edge emitting devices compared to the length of the external cavity L_{EC}, in the long external cavity regime typically longer than 10 cm. In the long cavity regime the frequency of the external cavity round trip $\tau_{EC} = c/2L_{EC}$ (¡¡ 1 GHz) is also significantly smaller than the relaxation oscillation frequency RO (1..10 GHz) of the SL. The ECSL is a delay system with a broad range of internal time scales featuring a strong nonlinearity, which is due to the strong amplitude phase coupling of the optical field in the SL. Such a system can exhibit an infinite number of possible degrees of freedom. Thus, the dynamics can become chaotic with a high-dimensional attractor and exhibit a broad bandwidth of frequencies. The time-delayed optical feedback induces a dynamical response of the laser which can cause an increase of the optical linewidth of the SL by a factor of about 1000 in conjunction with the emission dynamics becoming chaotic. This phenomenon is known as 'coherence collapse'. Experimentally the emission dynamics of the ECSL can be well-controlled by variations of different system parameters.
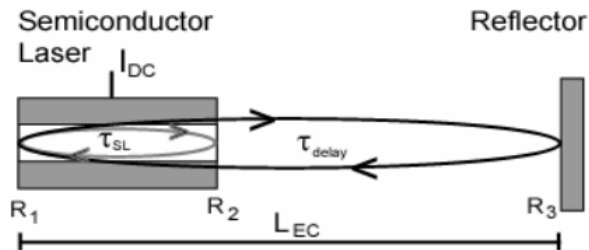

Figure 1. Scheme of a semiconductor laser subject to delayed optical feedback

A typical experimental setup used to investigate this all-optical chaos generator is depicted in Figure 2. It consists of an ECSL and several detection devices. The ECSL consists of an edge emitting SL which is driven by a low noise DC current source, a collimation lens, a variable neutral density filter VNDF and a high reflecting mirror with a reflectivity of approximately 99 % terminating the external cavity.
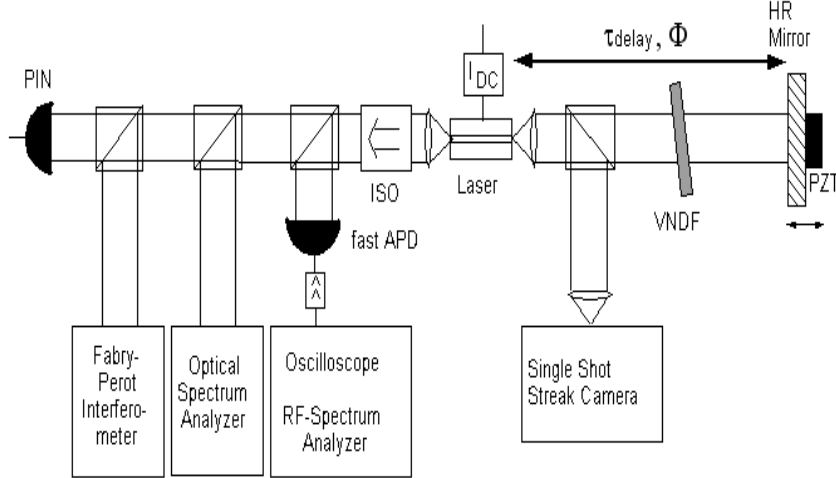
Figure 2. Typical experimental setup of all-optical transmitters with free-space external cavity

The SL is been cw-driven with constant injection current I_{DC}. Its emitted light is collimated by the collimation lens, and the feedback rate is controlled via the VNDF. The light is reflected from the mirror and finally reinjected into the SL. A setup providing sufficient mechanical robustness and control of the external cavity lengths with an accuracy of approximately 40 nm is introduced and realized using precision piezo transducers (PZT). Thus, the phase of the optical feedback can be controlled with respect to the phase of the optical field in the SL, shifting the length of the external cavity L_{EC} on sub-wavelength scale. In the long cavity regime the length of the external cavity ranges between 10 cm up to several meters and the power of the feedback is set to be within 1% and 10 % of the emitted power. Thus, the ECSL is driven in the moderate feedback regime.

A striking particularity of an ECSL operating in this regime is the wide range of temporal and spectral scales present in its dynamics. The broad range of temporal and spectral scales present in the system is highly demanding for the detection purposes. The optical spectrum is measured with a grating spectrometer (OSA) with a resolution of 0.05 nm resolving the longitudinal modes of the laser diode. The intensity dynamics of the system is detected with a fast photo detector with a bandwidth of 12 GHz. Its signal is amplified and analyzed by a fast digitizing oscilloscope with a temporal resolution limited to 4 GHz. Simultaneously, the signal is spectrally analyzed by an electrical spectrum analyzer (ESA) with a bandwidth of up to 12 GHz, limited by the photo detector. Additionally, a single-shot streak camera providing a resolution bandwidth of up to 100 GHz accounts for the even faster dynamics present in the system.

For the long cavity regime and for injection currents I_{DC} close to the threshold current of the solitary laser, the laser operates in the well-known Low Frequency Fluctuations (LFF) regime. This regime is characterized by sudden power dropouts followed by a slow recovery of the optical power. This regime, although interesting, is not very useful for chaos communications since information can be lost during the dropouts. For this reason, it is better to work at higher injection currents, at the fully developed coherence collapse regime. Figure 3 shows the intensity dynamics in the fully developed coherence collapse regime in two different time windows. Irregular pulsations on fast time scales (sub-nanosecond time scale) can be seen. In recent years it has been clarified that this dynamics is indeed chaotic with high dimensionality, thus being a candidate for chaotic carrier signals. Also the corresponding rf spectrum of the dynamics, depicted in Figure 4 exhibits chaotic characteristics.
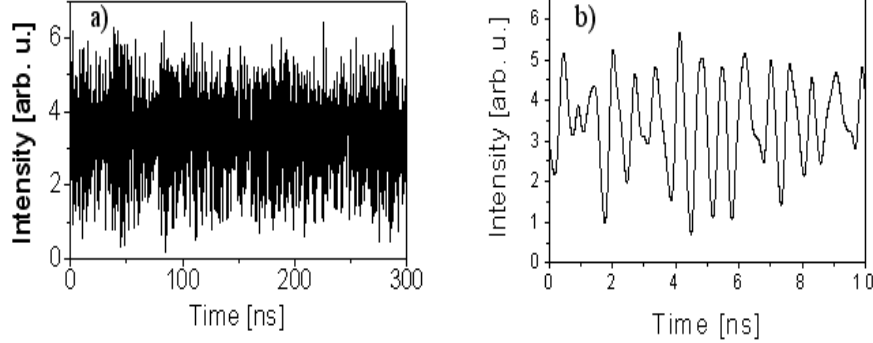
3

Figure 3. A 300 ns time slot of the emission dynamics for IDC = 1.3 Ith is depicted in panel a). The corresponding 10 ns zoom of the time series in a) is depicted in panel b).
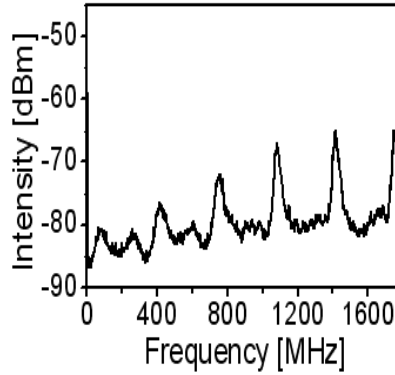

Figure 4. Rf spectrum for $I_{DC} = 1.3 \, I_{th}$ according to the time series depicted in figure 6

Figure 5 depicts autocorrelation functions for the dynamics within this regime. The autocorrelation function exhibits a fast first falloff of correlation within a few cavity roundtrips. The wings of enhanced correlation vanish to around 20 roundtrips. This property makes the higher pumping regime attractive for encoded data transmission, although it has to be mentioned that detection and characterization are more demanding in this regime: the bandwidth of the chaotic pulsations is higher and the dynamics is more complex.

Concentrating on the requirements concerning compactness, high bandwidth, flatness of the rf spectrum, and fast decreasing correlations, we have explored, whether further improvements compared to the previously discussed results can be achieved using short external cavities. Physically, there is one major difference when reducing the length of the external cavities, compared to the long cavity regime. In the short cavity regime the frequency of the external cavity round trip $\tau_{EC} = c/2L_{EC}$ becomes larger than the relaxation oscillation frequency RO (1..10 GHz) of the SL. Therefore, the dynamics exhibits different features and phenomena than in the long cavity regime. Furthermore, it has turned out, that the dynamical behavior is depending on the cavity phase of the delayed optical feedback field. This implies high requirements on the mechanical robustness which, however, can be fulfilled. For low pumping conditions the behavior can be switched between stable emission, quasiperiodic and irregular emission by varying the feedback phase.

Figure 8 shows the intensity dynamics, again in two different time windows, obtained for an injection current of $I_{DC} = 1.2 \, I_{th}$ and a length of the external cavity of $L_{EC} = 3.9$ cm. The dynamics comprises fast chaotic pulsations in the GHz range, thus being suited as chaotic carrier signal for communication experiments. The advantages of the short cavity regime become more clear when looking at the corresponding rf spectrum, depicted
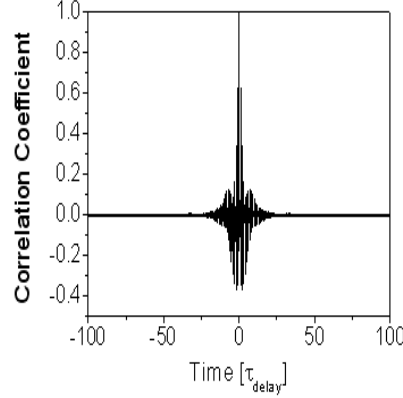
4

Figure 5. Autocorrelation function of the time series for $I_{DC} = 1.3\ I_{th}$. The time scale is normalized to the external cavity round trip time being 2.9 ns corresponding to $L_{EC} \sim 40$ cm.
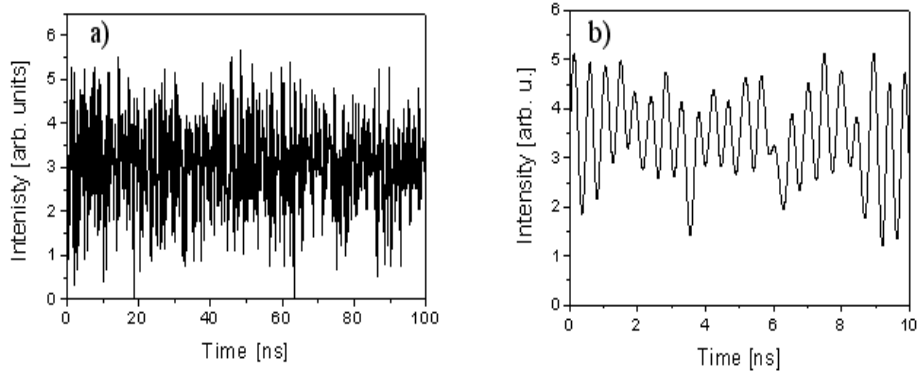

Figure 6. Intensity dynamics in the short cavity regime for $I_{DC} = 1.2\ I_{th}$ and $L_{EC} = 3.9$ cm a) 100 ns time window and b) 10 ns zoom of a)

in Figure 7. It shows ideal properties with almost flat spectrum up to the first external cavity resonance which can be easily shifted to about 10 GHz. Only a small falloff to low frequencies can be observed. Also the correlation properties of the dynamics in the short cavity regime show attractive properties for chaos communication. Figure 8 depicts a comparison of two autocorrelation functions, one for a 40 cm long cavity, as discussed previously, and one for a 3.9 cm short cavity.

The autocorrelation function for the dynamics in the short cavity regime decreases within the same number of cavity roundtrips, i.e. absolutely even faster than for the long cavity regime. The correlation vanishes within 15 roundtrips and shows no wings, as still present in panel a).

For the systems based on emitters, emitting chaotically due to delayed optical feedback, receiver systems in both configurations, closed loop and open loop have been studied. The major difference of this two configurations is that in the closed loop setup the receiver laser has a similar external cavity like the emitter system, in the open loop setup, the receiver system consists of the solitary laser without feedback. Figure 9 depicts a scheme of the experimental setup with the two sub-systems optically coupled via an optical isolator, $\lambda/2$ plate and a polarizer, in order to guarantee unidirectional coupling via the lasing TE component of the field. The optional cavity of the receiver system is depicted with a dashed line. Since well-matched parameters are essential for these synchronization experiments, we have selected two device-identical SLs. Their optical spectra agree within 0.1 nm, their slope efficiency within 3% and their threshold currents within 7%. Each laser is pumped by a low
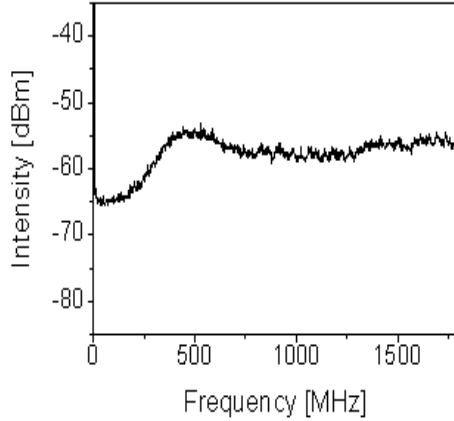
5

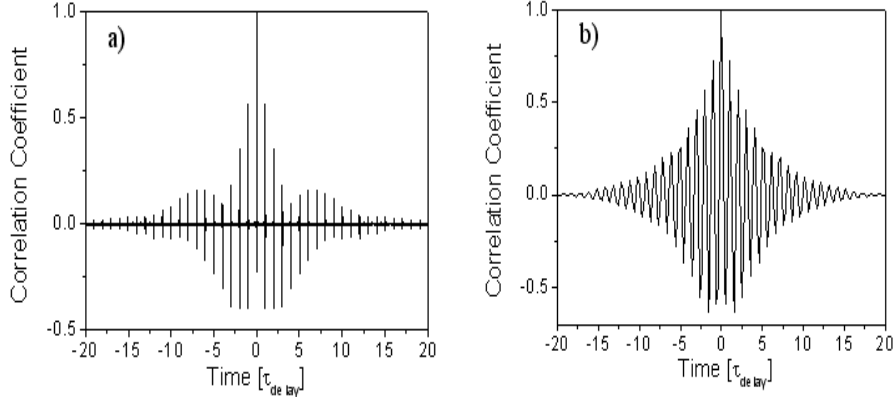**Figure 7.** Rf spectrum for $I_{DC} = 1.3\ I_{th}$ according to the time series depicted in figure 6

Figure 8. Autocorrelation functions of the intensity dynamics at IDC = 1.3 Ith a) for a 40 cm long external cavity, and b) for a 3.9 cm long external cavity. The time scales are normalized to the corresponding cavity round trip time τ_{delay}.

noise DC current source, and temperature stabilized to better than 0.01 K. The two systems are coupled via the injection of a well-defined fraction of the optical field of the emitter laser into the receiver system.

For the closed loop configuration a setup providing control of the external cavity lengths with an accuracy of approximately 40 nm has been introduced and realized using precision piezo transducers. This has turned out to be of decisive importance, since the relative optical phase $\Phi_{rel} = \Phi_T - \Phi_R$ of emitter and receiver cavities determines the synchronization properties of the receiver system. A detailed characterization for variation of this key parameter has been achieved. A characteristic synchronization scenario has been observed, leading from chaos synchronization to uncorrelated states and back to chaos synchronization, thus, pointing out this control parameter as crucial for the synchronization behavior of the receiver. Figure 10 depicts synchronized time series on two different time scales for matched cavity phases for the lasers operating in the coherence collapse regime. These synchronization properties are robust against reasonable detunings of several GHz and small parameter
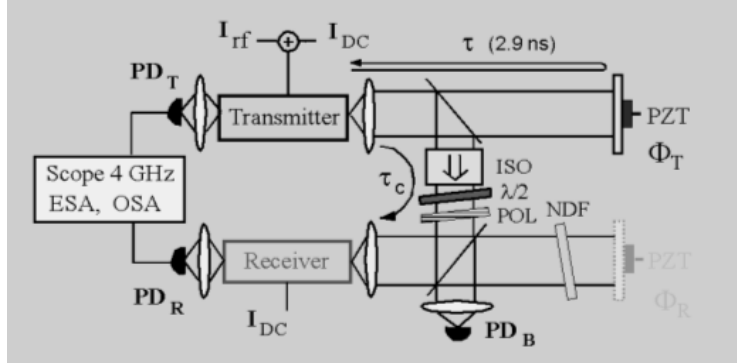
Figure 9. Setup of experiment with two unidirectionally coupled semiconductor laser systems in the all-optical scheme. For the receiver system closed loop and open loop configuration are depicted.

deviations of laser threshold and slope efficiency as indicated above. The obtained correlation coefficient is larger than 0.8.
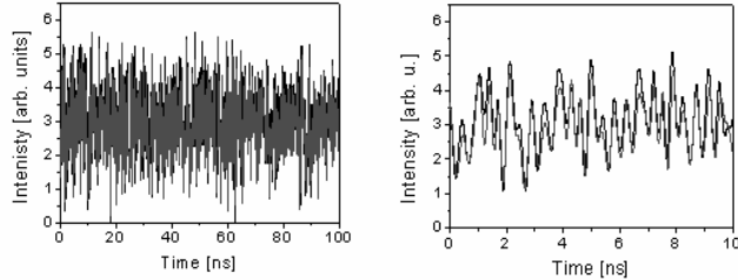

Figure 10. Time series of intensity dynamics of emitter (black) and receiver system (grey) in the coherence collapse regime for matched relative cavity phase.
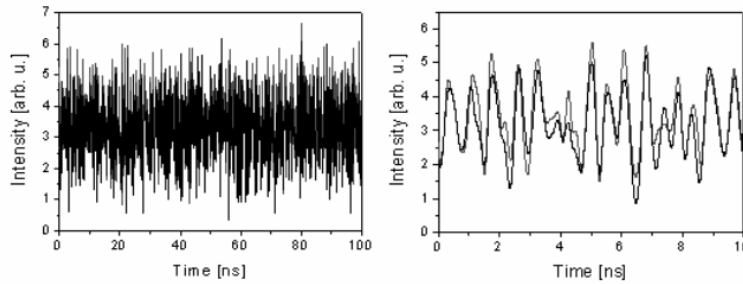

Figure 11. Time series of intensity dynamics of emitter (black) and receiver system (grey) in the coherence collapse regime for the open-loop configuration.

For the open loop configuration, the cavity of the receiver laser is been removed. In direct comparison to the experiments in the closed loop configuration, parts of the presented experiments have been performed using the same lasers and detection. Correlation coefficient as large as 0.8 are also obtained. Consequently, both configurations exhibit attractive features for the utilization in chaos communication systems. When encoding a signal, both schemes exhibit high signal/carrier discrimination of up to 15 and 20 dB, respectively, and a frequency range which extends into the desired GHz range. The limitation to 2 GHz in these experiments was technically caused, so that an extension to even higher frequencies appears possible. The differences of these two

7

schemes are slightly better synchronization and chaos pass filtering in the closed loop scheme which is however contrasted by higher mechanical robustness, simpler and cheaper setup of the open loop configuration.

3. EMITTER AND RECEIVERS SUBJECT TO ELECTRO-OPTICAL FEEDBACK

With the configuration reported below, the intensity (-or amplitude) of a semiconductor laser is made to fluctuate chaotically around a mean value. The message is masked as a small intensity modulation with a masking efficiency which of the order of -15 dB in the experiments reported so far. The experimental set-up used is schemed in figure 12. The laser diode is a conventional CW DFB laser operating at 1550 nm. The nonlinearity in the feedback loop comes from the electro-optic Mach-Zehnder interferometer. First experiments have been performed up to 150 MHz for demonstration purposes, although the bandwidth can be extended by changing some of the components.
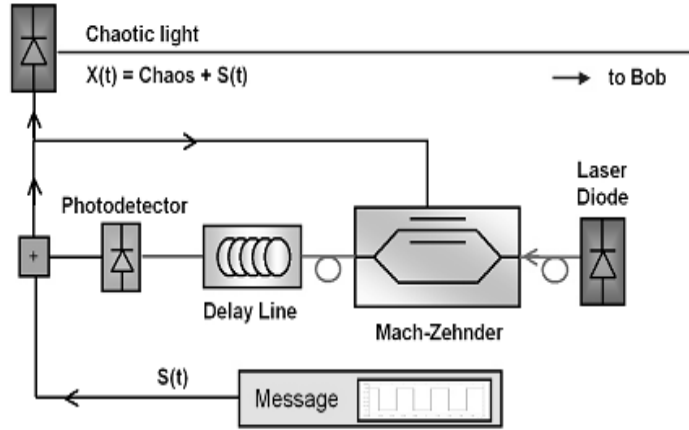

Figure 12. Transmitter with optoelectronic feedback for the generation of chaos in intensity

The emitter comprises the following components: A CW DFB MQW laser diode emitting at a wavelength of 1550 nm. This light source optically powers the electro-optic modulator. An electro-optic modulator, the integrated LiNbO3 Mach-Zehnder Interferometer (MZI). This X-cut modulator has transmission specifications of 2,5 Gbits/s at 1540 nm. Its half-wave voltage is of 3.6 Volts (in TM mode) and can take up to 1W electrical input power. This modulator has a driving voltage X(t) which goes up to 11V, 3 times the half-wave voltage in order to operate in the non-linear modulation regime. The DC bias voltage is in 7. 3. A fibre optic cable is inserted in between the modulator and the photodetector in order to introduce a time delay of T = 50 ns. This fibre is therefore used as a time delay line. A photodetector which detects the intensity modulation $I_S(t)$ introduced by the MZI on the light beam produced by the previous device. A feedback loop. Its purpose is to feed the electrical signal V(t) detected by the photodetector onto the driving electrodes of the MZI after filtering with a 1 GHz bandpass filter centred at 600 MHz. A RF amplifier of gain 20 dB. A DC source to provide bias voltage for the MZI. An output line for acquisition purposes of the chaotic signal X(t).

The complete set of the dynamics that we can produce is seen on a bifurcation diagram of figure 13, which represents the values taken by X(t) for different values of the bifurcation parameter. In our case, we have the optical power of the laser diode vary. Figure 13 is an example of a bifurcation diagram. The data was obtained experimentally at the output of the chaos generator. We have chosen to have a TM type polarization at the input of the MZI. The bifurcation diagram shows a great number of dynamical regimes that we can observe before reaching the zone where we can create chaos. We can see that four zones stand out in diagrams of figure 13. The first zone (bifurcation parameter value between 3-4.5 mW) is the one of periodic dynamics. The second one (bifurcation parameter value between 4.6-6.6 mW) corresponds to complex structures whose spectrum is
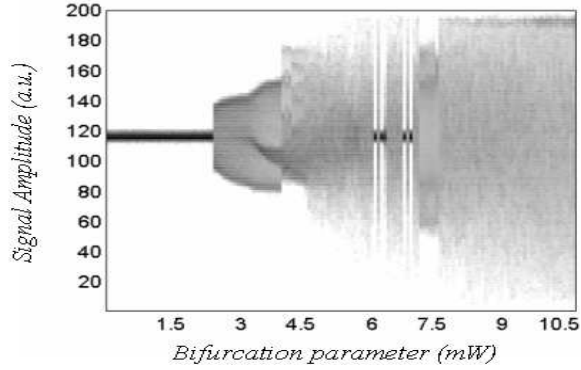
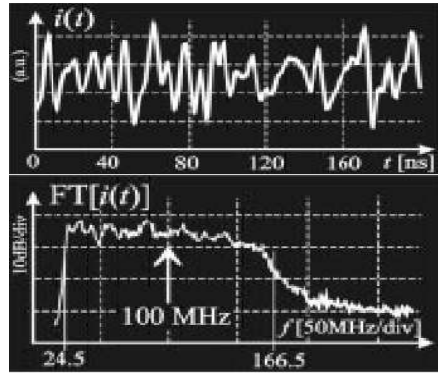**Figure 13.** Experimental bifurcation diagram.

Figure 14. Time trace of the output power (upper panel) and Rf spectrum (lower panel) for the system operating in a chaotic regime.

composed of both a continuous part and rays. The continuous part in the spectrum is linked to the apparition of chaos. The third zone (bifurcation parameter value between 6.7-7.5 mW) is a part of the diagram where the dynamics of the system are not stable. The fourth zone of the diagram starts with multiple complex structures. This is followed by a sub-zone where the structure of the dynamic regime tends to disappear. These two sub-zones are chaotic in nature. The one that interests us for our system is the last one (bifurcation parameter value between 7.6-11.3) where the Gaussian white noise chaos is fully developed. Figure 14 shows a time trace and its spectrum when operating into the fully developed chaos region. Both the time trace of the optical power and the flat spectrum confirm the chaotic nature of the output. With this in mind, we can then test our system when inserting a message into the chaos feedback loop.

In figure 15 shows the experimental setup for open loop and parameter matching. The top branch in the diagram of figure 15 is used as a reference, equivalent to the emitter while the other branch is the slave and is analog to the receiver. The receiver is symmetrically designed, as it can be noticed. The main difference relies in the open loop architecture, which was shown to be the best configuration for the optoelectronic set-up. The open loop architecture involves an RF power divider after the optoelectronic detection of the received encrypted optical beam, and an RF subtracter to retrieve the locally generated chaotic signal from the detected one. In figure 16we show the synchronization diagram, i.e. we plot the output of the emitter vs. the output of the receiver. The 45 line indicates perfect synchronization. Although no perfect, the achieved synchronization quality is good enough.
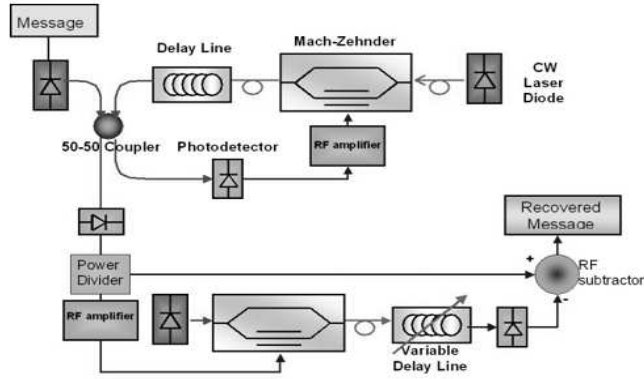
Figure 15. Emitter/receiver optoelectronic chaos-based encryption System.
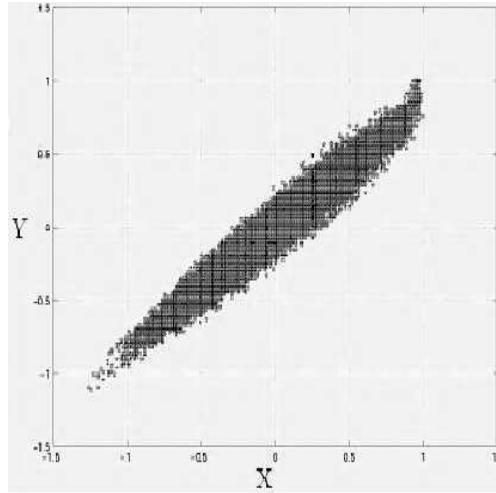

Figure 16. Synchronization diagram.

So far, the gains of the systems have been matched easily tuning the CW optical power of the laser, or/and the electrically tunable gain of the RF drivers. The time delay has to be much more accurately matched (within a few 0.01%), which is obtained thanks to an optical delay line. The latter consists in a collimated free space beam coming from, and going to fiber ends. The free space path can be accurately adjusted through a micrometer positioning system, thus producing a highly accurate time delay on a 10 cm tuning range. The receiver fiber delay line is initially cut at a length within the tuning range of the tuning optical delay line. Testing the delay is performed by scanning the driving signal frequency from a few MHz, where both outputs are superimposed on the oscilloscope screen, up to 4GHz, which corresponds to the oscilloscope bandwidth. The sine waveforms keep in phase for the whole frequency range explored, indicating that the delay matching is good. Within this configuration a high correlation coefficient between the emitter and receiver output is obtained (larger than 0.9).

4. CONCLUSIONS

In this paper we have reported the realization and characterization of chaotic transmitter/receiver systems suited for encoded GBit/s communication systems. We have defined requirements for the transmitter systems and

10

evaluated the different configurations and modes of operation. All optical and electro-optical feedback devices were analyzed. It has been observed that both systems develop, under appropriate conditions, high dimensional chaotic outputs.

The all-optical transmitters/receivers with long extended cavities operation in the fully developed coherence collapse regime exhibits distinctly good properties. In particular, the correlation properties are good, bandwidth is large, and at the same time good synchronization properties can be maintained. This system is a good candidate for a Gbit/s chaos communication experiments. Parallel to the long external cavities, setups with short external cavities have been realized. It has been found that even better properties than for long cavity configurations can been obtained. In particular, they offer more compactness, even faster correlation falloff compared to long cavities, and almost white rf spectra. Receiver with open and closed loop configurations have been considered. Slightly better performances were observed in the closed loop system.

The electro-optical transmitters/receivers operating in the chaotic regime exhibits good correlation properties, large spectral bandwidth and good synchronization properties. The open loop configuration in the receiver exhibits much better performances than the closed one (not described in this paper).

Both systems allow for encoding messages at Gbit/s rates if suitable components are used in both emitter and receiver subsystems.

ACKNOWLEDGMENTS

REFERENCES

1. L. M. Pecora and T. L. Carroll *Phys. Rev. Lett.* **64**, p. 821, 1990.
2. K. M. Cuomo and A. V. Oppenheim *Phys. Rev. Lett.* **71**, p. 65, 1993.
3. C. R. Mirasso, P. Colet, and P. Garcia-Fernandez *IEEE Phot. Tech. Lett.* **8**, p. 299, 1996.
4. G. D. VanWiggeren and R. Roy *Science* **279**, p. 1198, 1998.
5. L. Larger, J. P. Goedgebuer, and F. Delorme *Phys. Rev. E* **57**, p. 6618, 1998.
6. S. Sivaprakasam and K. A. Shore *Optics Lett.* **24**, p. 466, 1999.
7. I. Fischer, Y. Liu, and P. Davis *Phys. Rev. A* **62**, p. 011801, 2000.
8. *Feature Section on Optical Chaos and Applications to Cryptography*, vol. 38, Ed. by S. Donati and C. R. Mirasso, IEEE J. Quantum Electron., 2002.
9. F. Rogister, A. Locquet, D. Pieroux, M. Sciamanna, O. Deparis, P. Megret, and M. Blondel *Phys. Rev. E* **58**, p. 1486, 1998.
10. S. Tang, H. F. Chen, and J. M. Liu *Optics Lett.* **26**, p. 1489, 2001.